J Mater Sci: Mater Electron (2013) 24:2659–2666
DOI 10.1007/s10854-013-1152-z

A comprehensive study on mechanical properties of $Bi_{1.8}Pb_{0.4}Sr_2Mn_xCa_{2.2}Cu_{3.0}O_y$ superconductors

M. Dogruer · F. Karaboga · G. Yildirim · C. Terzioglu · O. Ozturk

Received: 10 January 2013 / Accepted: 20 February 2013 / Published online: 2 March 2013

Abstract This study manifests the crucial change in the mechanical performances of $Bi_{1.8}Pb_{0.4}Sr_2Mn_xCa_{2.2}Cu_{3.0}O_y$ superconductor samples (x = 0, 0.03, 0.06, 0.15, 0.3 and 0.6) prepared by conventional solid-state reaction method by use of Vickers microhardness (H_v) measurements carried out at different applied loads, ($0.245\ N \leq F \leq 2.940\ N$). Load dependent microhardness, load independent microhardness, Young's (elastic) modulus and yield strength values being account for the potential technological and industrial applications are evaluated from the hardness curves and compared with each other. It is found that the H_v, elastic modulus and yield strength obtained decrease (increase) with the enhancement of the applied load for the undoped (doped) samples. Surprisingly, the results of the H_v values illustrate that the samples doped with x = 0.03, 0.06, 0.15, 0.3 and 0.6 exhibit reverse indentation size effect (RISE) feature whereas the pure sample obeys indentation size effect (ISE) behavior. Furthermore, the experimental results are examined with the aid of the available methods such as Meyer's law, proportional sample resistance model (PSR), elastic/plastic deformation (EPD), Hays–Kendall (HK) approach and indentation-induced cracking (IIC) model. The results inferred show that the hardness values calculated by PSR and EPD models are far from the values of the plateau region, meaning that these models are not adequate approaches to determine the real microhardness value of the Mn doped Bi-2223 materials. On the other hand, the HK approach is completely successful for the explanation of the ISE nature for the pure sample while the IIC model is obtained to be the best model to describe the hardness values of the doped materials exhibiting the RISE behavior. Additionally, the bulk porosity analysis for the samples reveals that the porosity increases monotonously with the increment in the Mn inclusions inserted in the Bi-2223 system, presenting the degradation of the grain connectivity.

M. Dogruer (✉) · F. Karaboga · G. Yildirim · C. Terzioglu
Department of Physics, Abant Izzet Baysal University, Bolu 14280, Turkey
e-mail: musadoqruer@gmail.com

G. Yildirim
Department of Mechanical Engineering, Abant Izzet Baysal University, Bolu 14280, Turkey

O. Ozturk
Department of Physics, Kastamonu University, Kastamonu 37100, Turkey

1 Introduction

The microhardness, elasticity, ductility and toughness of materials are very crucial mechanical parameters for industrial applications in the form of wires and tapes. However, the applications of high temperature (type-II) superconductor ceramics such as YBCO and BSCCO are usually restricted owing to their brittleness behavior and thus researchers have endeavored to improve the mechanical properties of BSCCO materials for years.

Microhardness measurements enable the researches to express the mechanical properties of the different sort of materials such as ceramics, thin films, alloys, semiconductors, polymers and especially superconductors [1–3]. Besides, these measurements with harmless and easy procedure are commonly used to determine the quality of generated superconductors in the industry [4–6]. For example, in the literature, Terzioglu [7] analyzed the effect on physical properties of Gd added Bi-2223 superconductors and found that Gd addition level reduces the microhardness of the samples. This degradation stems from the enhancement of

the voids, impurity phase segregation and the modification of the grain boundaries. Kolemen et al. [8] examined the role of Sm-substitution on the Vickers microhardness (H_v) of Bi-2223 ceramics. This group explained that Meyer's law failed to define the change in the microhardness with the applied load. Cavdar et al. [9] also investigated the role of PbSe inclusions on mechanical properties of the Bi-2212 ceramics and reported that the microhardness values increase with enhancing the addition of PbSe for glass samples as well as decreasing for the superconducting samples. Awad et al. [10] studied the mechanical properties of $(Cu_{0.5}Tl_{0.5})$-1223 substituted by the rare earth metal of Pr and observed that Hays–Kendall (HK) approach, elastic/plastic deformation (EPD) and proportional specimen resistance model failed to examine the reverse indentation size effect (RISE) nature. On the other hand, they also found that the indentation-induced cracking (IIC) model was best fitted for $Cu_{0.5}Tl_{0.5}Ba_2Ca_{2-x}Pr_xCu_3O_{10-\delta}$ samples. Dogruer et al. [11] investigated H_v of $YBa_2Cu_{3-x}Gd_xO_{7-d}$ superconducting ceramics. According to the experimental results reported, the microhardness values improve with the enhancement of the Gd inclusions in the Y123 ceramics as a consequence of the increment in the strength of the bonds between grains.

In this work, we manifest the influence of the mechanical properties of Mn inclusions in the Bi-2223 systems by way of H_v measurements. The obtained results of the hardness measurements are studied by different models such as Meyer's law, proportional sample resistance model (PSR), EPD, HK approach and IIC model. It is found that the HK approach is the best model for defining the microhardness properties of the pure sample while the IIC model is obtained to be the best model to explain the microhardness values of the Mn doped Bi-2223 bulk samples. Furthermore, we compute porosity values inferred from the density results to discuss the relationship between the mechanical properties and grain connectivity between superconducting grains.

2 Experimental details

In previous work, we examined the effect of Mn addition on electrical, structural, physical and superconducting properties of the Bi-2223 superconductors by use of bulk density, resistivity (ρ-T), X-ray diffraction analysis (XRD), scanning electron microscopy (SEM), transport critical current density (J_c) and electron dispersive X-Ray (EDX) measurements in detail [12]. Further, the flux pinning mechanism properties were studied for the characterization of the samples in the applied magnetic fields range of 0–7 T [13]. In this study, the role of Mn inclusions in Bi-2223 matrix on mechanical properties is analyzed via H_v measurements in air using a SHIMADZU HVM-2 model digital microhardness tester at the room temperature. The applied load is changed from 0.245 to 2.940 N for a loading time of 10 s and accuracy in the determination of indentation diagonals is defined as ±0.1 μm. The experiment results are recorded at the different locations on the specimen surface to avoid the surface effects and work hardening. An average of ten readings at different locations of the specimen surfaces is taken for reasonable mean values. In the present work, the undoped sample is demonstrated as Mn0 whereas the superconductor samples produced with different Mn content such as 0.03, 0.06, 0.15, 0.3 and 0.6 will be herein after presented as Mn1, Mn2, Mn3, Mn4 and Mn5, respectively. Furthermore, the porosity values for all the samples are deduced from the density results in [12] and the strength of connection between superconducting grains is discussed in detail.

3 Results and discussion

Previously, we investigated the electrical, physical, microstructural and superconducting properties of the samples and reported that the zero-resistivity transition temperature and transport critical current density decreased with the increment of Mn inclusions in Bi-2223 matrix. As for the XRD results, the lattice constants *a* increased while the *c* parameter decreased with the Mn additives. Additionally SEM results illustrated that the surface morphology and grain connectivity degraded with the addition due to the decrement of the grain sizes. Moreover, EDX measurements showed that not only do the Sr and Cu compositions in the samples compared to other element compositions reduce with the Mn addition but the elements used for the preparation of samples are homogeneously distributed, as well. In addition, the bulk density was found to decrease at a constant rate with the increase of Mn inclusions inserted in the Bi-2223 ceramics [12]. Also, we examined the flux pinning mechanism properties with the aid of the activation energies, irreversibility and upper critical fields in the applied magnetic fields range from 0 to 7 T. It was concluded that the Mn addition forced the pinning ability of the Bi-2223 materials to reduce due to the pair-breaking mechanism [13]. In the present study, the change of mechanical properties with the Mn concentration level in Bi-2223 system is analyzed by H_v measurements. We also use a number of models to explain the indentation size effect (ISE) and RISE feature in the samples prepared.

3.1 Microhardness and modeling

Measurement of the diagonal length against a test load allows us to describe the mechanical properties of a material. In this work, we determine the influence of the Mn inclusions on the mechanical properties of Bi-2223

samples by measuring the diagonal length. The H_v values of different applied loads in the range from 0.245 to 2.940 N can be evaluated from the following equation:

$$H_V = 1854.4\left(\frac{F}{d^2}\right) \quad (1)$$

The measured indentation diagonal lengths (d) and computed microhardness values (H_v) using Eq. (1) for different applied loads (F) are visualized in Table 1. As can easily be seen in the table, the microhardness values for all the samples depend strongly on the applied indentation loads. The change of load dependent microhardness with the applied loads for undoped and Mn doped Bi-2223 materials is presented in Fig. 1. One can see from the figure that the samples studied in this work demonstrate two different behaviors to be identified as ISE [14] and RISE [15]. The pure sample exhibits the ISE behavior being attributed to the fact that the load dependent hardness values decrease non-linearly as the applied load increases up to 2.0 N after this point the curves shift to the saturation (plateau) region. The change in the curves is due to the grain boundary weak-links, specimen cracking/porosity, disorder, impurity phases and irregular grain orientation distribution [16]. The doped samples show RISE feature explaining the increment in the microhardness values with enhancement of the applied load. This may lead to the degradation in strength of connection between superconducting grains.

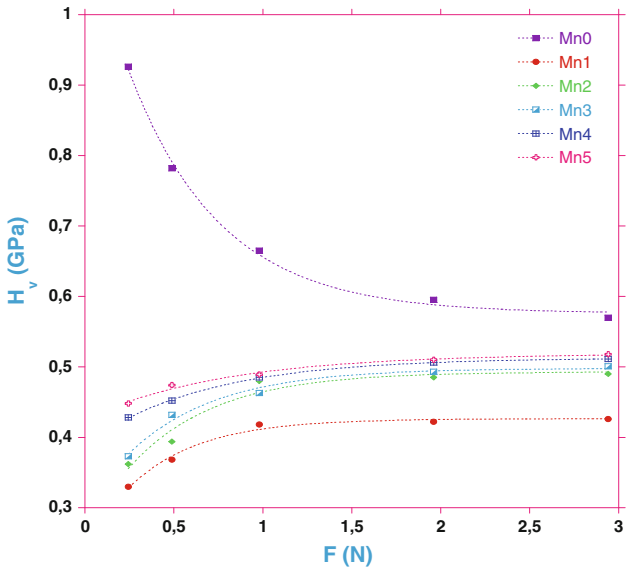

Fig. 1 Variation of microhardness value with applied load for all samples

Table 1 The calculated load dependent Hv, E and Y for the samples produced

Samples	d (μm)	Hv (GPa)	E (GPa)	Y (GPa)
Mn0	22.15	0.926	75.898	0.308
	34.11	0.782	64.095	0.260
	52.32	0.665	54.505	0.221
	78.26	0.595	48.768	0.198
	97.85	0.570	46.719	0.190
Mn1	37.10	0.330	27.048	0.110
	49.68	0.368	30.163	0.122
	65.93	0.418	34.261	0.139
	92.81	0.422	34.589	0.140
	113.13	0.426	34.916	0.142
Mn2	35.42	0.362	29.671	0.120
	48.02	0.394	32.294	0.131
	61.53	0.480	39.342	0.160
	86.57	0.485	39.752	0.161
	105.48	0.490	40.162	0.163
Mn3	34.89	0.373	30.572	0.124
	45.85	0.432	35.408	0.144
	62.65	0.463	37.949	0.154
	85.86	0.493	40.408	0.164
	104.32	0.501	41.064	0.167
Mn4	32.57	0.428	35.080	0.142
	44.83	0.452	37.048	0.150
	61.21	0.485	39.752	0.161
	84.75	0.506	41.474	0.168
	103.30	0.511	41.883	0.170
Mn5	31.84	0.448	36.720	0.149
	43.78	0.474	38.851	0.158
	60.96	0.489	40.080	0.163
	84.42	0.510	41.801	0.170
	102.59	0.518	42.457	0.172

Further, the elastic (Young's) modulus (E) and yield strength (Y) can be calculated from the following equations given below:

$$E = 81.9635H_V \quad (2)$$

$$Y \approx \frac{H_V}{3} \quad (3)$$

The results calculated are presented in Table 1. It is clear from the table that all the values found are related to both the applied load and Mn addition level. Young's modulus and yield strength values are obtained to decrease with the applied load for the undoped sample exhibiting the ISE feature but increase for the doped samples obtaining RISE nature. In addition, we use 5 different models such as Meyer's law, PSR, EPD, HK approach and IIC model to calculate the load independent hardness values and describe the ISE and RISE features belonging to the samples studied.

3.1.1 Meyer's law

Meyer's law is one of the reliable and useful methods to describe the mechanical characters of a material and the formula given below is identified:

$$F = A_1 d^n \tag{4}$$

where the power n denotes the Meyer number when A_1 presents the standard microhardness constants. The n value helps us to determine the ISE and RISE behavior of the material studied. The microhardness values decrease with ascending the applied load (ISE) as $n < 2$ but increase when $n > 2$ (RISE). On the other hand, when $n = 2$, it is well known that Kick's law is valid ($F = A_1 d^2$). For our samples, the n and A_1 values found from linear ln F versus ln d (Fig. 2) curves are listed in Table 2. The results obtained display that the n values are found to be <2 for the pure sample because of the ISE nature, while the doped samples show RISE behavior as a consequence of the Meyer number [17].

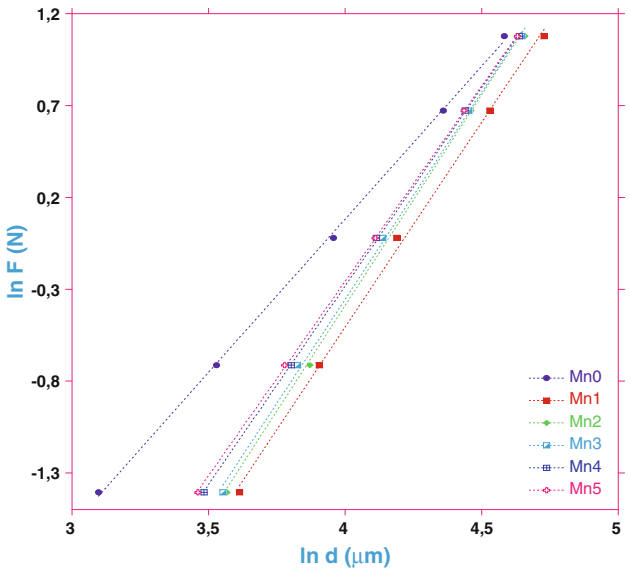

Fig. 2 Variation of applied load ln F with diagonal ln d for the samples

3.1.2 PSR model

Proportional sample resistance model is preferred to determine easily the ISE or RISE feature of a material with the aid of the following formula [18–20]:

$$\frac{F}{d} = \alpha + \beta d \tag{5}$$

where the parameter α presents the surface energy and the variation in α value is related with the energy dispersion of the surface cracks. Using the β parameter values, the load independent microhardness value is calculated by the available relation:

$$H_{\mathrm{PSR}} = 1854.4\beta \tag{6}$$

The parameters of α and β can be extracted from the linear graphs of F/d versus d (Fig. 3) for the Mn doped Bi-2223 superconductors (Table 2). It is obvious from the table that the α is positive, confirming that the pure sample demonstrates the ISE nature while the surface energy (α) is negative for the doped samples showing RISE feature, presenting that the plastic deformation is superior to the elastic deformation in the samples. Further, the obtained H_{PSR} values are reported in Table 3. As seen from the table that the load independent microhardness values computed by the PSR model are far from the load dependent hardness value (plateau region). Hence, it is not wrong to say that the PSR model is not sufficient for the determination of the original microhardness value of the Mn doped Bi-2223 materials.

3.1.3 EPD model

Elastic/plastic deformation is another model to discuss the ISE and RISE behavior of a material. In this model, the dependence of indentation size on the applied load is calculated by the formula [21]:

Table 2 The calculated parameters according to different models for Bi-2223 system

Samples	Meyer's law		PSR model		EPD model		HK model		IIC model	
	$A_1 \times 10^{-4}$ (N/μm^2)	n	$\alpha \times 10^{-2}$ (N/μm)	$\beta \times 10^{-3}$ (N/μm^2)	d_e (μm)	A_2 (N/μm^2)	W (N)	$A_3 \times 10^{-5}$ (N/μm^2)	$K \times 10^4$ (N$^{(3-5mA)/3}$/μm$^{(2-3m)}$)	m
Mn0	13.740	1.66	0.57	0.248	0.14	0.0161	0.139	29.44	1825.5	1.44
Mn1	0.810	2.22	−0.26	0.254	−0.09	0.0160	−0.074	23.60	0.0026	0.33
Mn2	0.704	2.29	−0.36	0.302	−0.12	0.0175	−0.101	27.43	0.0046	0.37
Mn3	0.843	2.25	−0.34	0.304	−0.10	0.0175	−0.101	27.92	0.0033	0.34
Mn4	1.336	2.15	−0.22	0.298	−0.07	0.0173	−0.066	28.17	0.0013	0.26
Mn5	1.600	2.12	−0.18	0.296	−0.05	0.0172	−0.056	28.38	0.0008	0.22

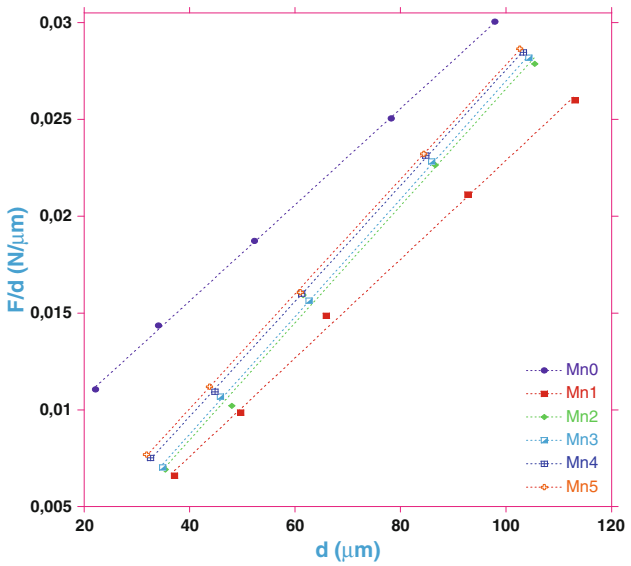

Fig. 3 Plots of F/d versus d for the samples studied

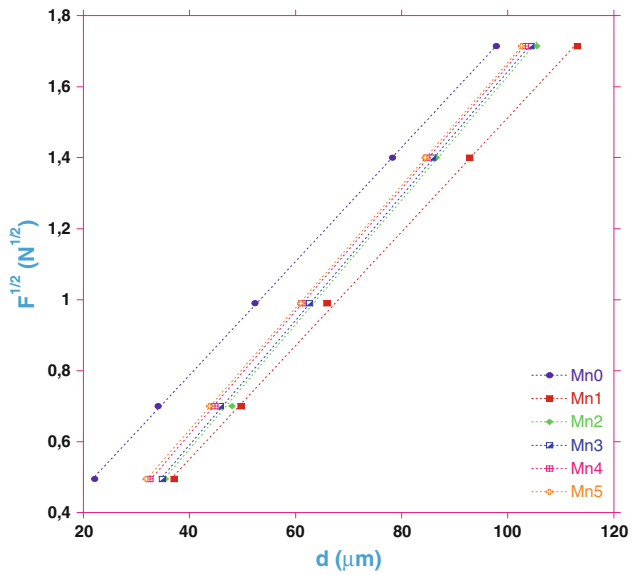

Fig. 4 Plots of square root of applied loads versus diagonal length for the samples

Table 3 The results of calculated values of H_V, H_{PSR}, H_{EPD}, H_{HK} and H_{IIC} model

Samples	H_{PSR} (GPa)	H_{EPD} (GPa)	H_{HK} (GPa)	H_{IIC} (GPa)	H_V (GPa)
Mn0	0.459	0.480	0.545	0.812	0.570–0.595
Mn1	0.471	0.474	0.437	0.393	0.422–0.426
Mn2	0.560	0.567	0.508	0.447	0.485–0.490
Mn3	0.563	0.567	0.517	0.472	0.493–0.501
Mn4	0.552	0.555	0.522	0.515	0.506–0.511
Mn5	0.548	0.548	0.526	0.525	0.510–0.518

$$F = A_2\left(d_e + d_p\right)^2 \tag{7}$$

where A_2 denotes the load independent microhardness constant when the elastic deformation (d_e) is associated with (d_p) plastic deformation. The linear graphs of $F^{1/2}$ versus d_p for the $Bi_{1.8}Pb_{0.4}Sr_2Mn_xCa_{2.2}Cu_{3.0}O_y$ superconductors are visualized in Fig. 4. The values of A_2 and d_e are gathered in Table 2. One can see from the table that the d_e is obtained to be positive only for the undoped sample showing the ISE nature. On the other hand, the obtained d_e values are found to be negative for the Mn doped samples, confirming that the plastic deformation is more dominant than elastic deformation in the ceramics. This may be attributed to the fact that the doped samples are obeying the RISE feature. Further, the load independent microhardness value can be defined by equation:

$$H_{\mathrm{EPD}} = 1854.4A_2 \tag{8}$$

It is seen that similar to the results of the PSR models, the load-independent microhardness (H_{EPD}) values of the samples are found to be changeable for the samples produced (Table 3). Additionally, Table 3 assures that the EPD model is not adequate for the determination of the real microhardness value.

3.1.4 HK approach

According to Hays–Kendall (HK) approach, there is a minimum test load (W) above which the plastic deformation begins to play more dominant role as compared to the elastic deformation in a material. If the test load is below the minimum value, the elastic deformation only occurs in the material [22]. Thus, the indentation size measured being the proportional to an effective load $F_{eff} = F - W$ instead of the applied load (F) can be found by the following equation:

$$F - W = A_3 d^2 \tag{9}$$

where A_3 presents the hardness constant. The H_{HK} can be computed by use of the following equation:

$$H_{HK} = 1854.4A_3 \tag{10}$$

The A_3 and W parameters are extracted from the linear graph $F - d^2$ as illustrated in Fig. 5. The obtained values of HK parameters are tabulated in Table 2. It is obvious that the values of W are positive for the pure sample illustrating ISE behavior. This may be described that the applied load is sufficient to produce both elastic and plastic deformation in the material. One can see from Table 3, the load independent microhardness values calculated from HK approach are closer to load dependent microhardness values (plateau region) when compared to other models. Consequently, the HK approach is the most suitable model

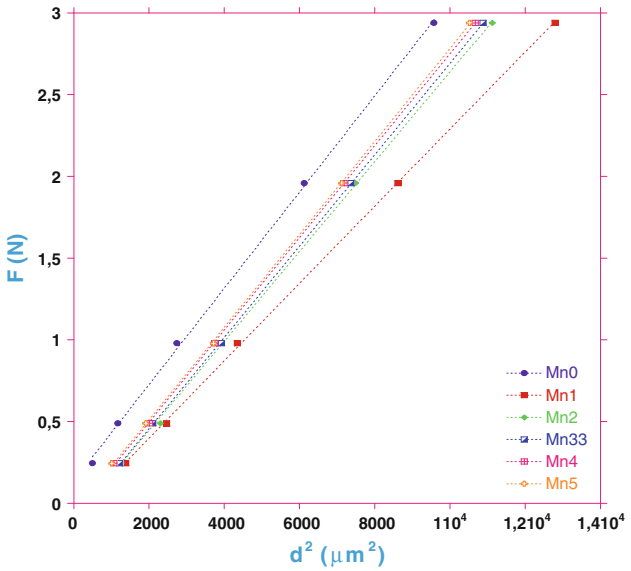

Fig. 5 Applied load versus the square of the impression length for the samples prepared

to describe the mechanical properties of the pure sample. As for the negative value of W, the applied load is enough to generate both the elastic and plastic deformation in the material studied. In this study, the plastic deformation as well as the elastic one is observed for the doped samples displaying the RISE feature as a result of the negative W values. Therefore, it is apparent that HK approach is inadequate for the explanation of the original microhardness values of the Mn doped Bi-2223 materials.

3.1.5 IIC model

The IIC model enables us to examine the RISE behavior of different superconductor systems [23]. In this model, the applied indentation test load is balanced by the total specimen resistance at the maximum depth consisting of four components:

- The friction at the indenter or specimen facet interface;
- Elastic deformation;
- Plastic deformation;
- Specimen cracking.

According to IIC model, indentation cracking contributes to the RISE behavior while frictional and elastic effects lead to the ISE feature of the samples produced in this work. The load independent microhardness value (H_{IIC}) can be calculated by use of the following relation:

$$H_v = \lambda_1 K_1 \left(F/d^2\right) + K_2 \left(F^{5/3}/d^3\right) \quad (11)$$

where d represents the indentation size when λ_1 denotes constants. K_1 is related with the geometry of the indenter whereas K_2 depends on the applied load. For an ideal perfect plastic material $H_v = K_1\,(F/d^2)$, $\lambda_1 = 1$ and $K_2\,(F^{5/3}/d^3) = 0$. For the perfect brittle solids $H_v = K_2\,(F^{5/3}/d^3)$ and $\lambda_1 = 0$. From the Eq. (11), the indentation diagonal can be taken as $d = 7h$ where h presents the indentation depth. This equality is in accordance with the angle (148°) between the opposite sides of the indenter. Thereby, the load independent microhardness values can be found from second term of the Eq. (11):

$$H_v = K\left(\frac{F^{5/3}}{d^3}\right)^m \quad (12)$$

The constant values of K and m are summarized in Table 2. Furthermore, the dependence of ln H_v on ln $(F^{5/3}/d^3)$ for the undoped and Mn doped Bi-2223 system is illustrated in Fig. 6. For $m > 0.6$ the sample exhibits ISE nature, whereas for $m < 0.6$ the sample shows RISE behavior. One can see from Table 2 that the m value is >0.6 for the pure sample. This may be attributed the fact that the undoped sample obeys ISE behavior. On the other hand, for the Mn added Bi-2223 superconducting samples, the m values are smaller than 0.6, confirming that the doped samples display the RISE feature. At the same time, it is noted that there exists empirical relation between the K and m as visualized in Fig. 7. The results in the figure are well fitted according to equation:

$$K = 0.541e^{12.03m} \quad (13)$$

In this work, we use 5 various models such as Meyer's law, PSR, EPD, HK and IIC models to analyze the microindentation results of the Bi-2223 ceramics. As reported in Table 3, the HK approach is successful for the depiction of

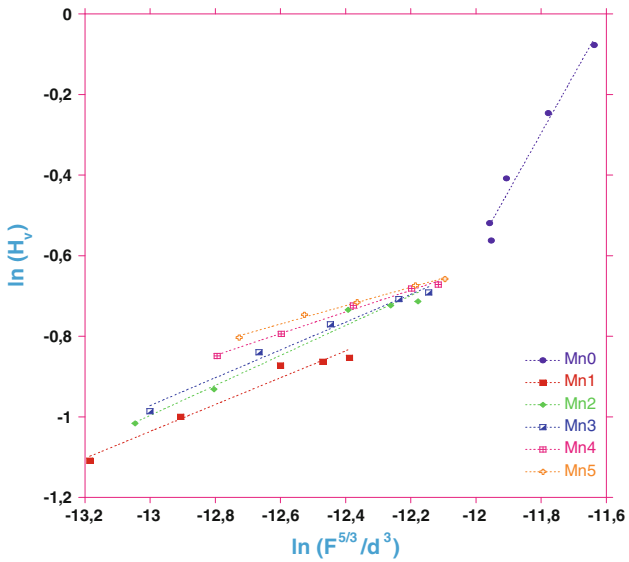

Fig. 6 Variation of ln H_V with ln $(F^{5/3}/d^3)$ according to *IIC* model for all samples

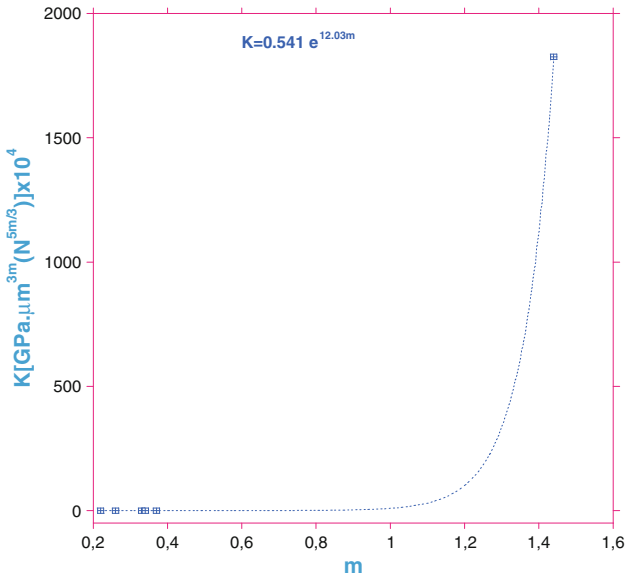

Fig. 7 The correlation between the IIC model parameters K and m for all samples

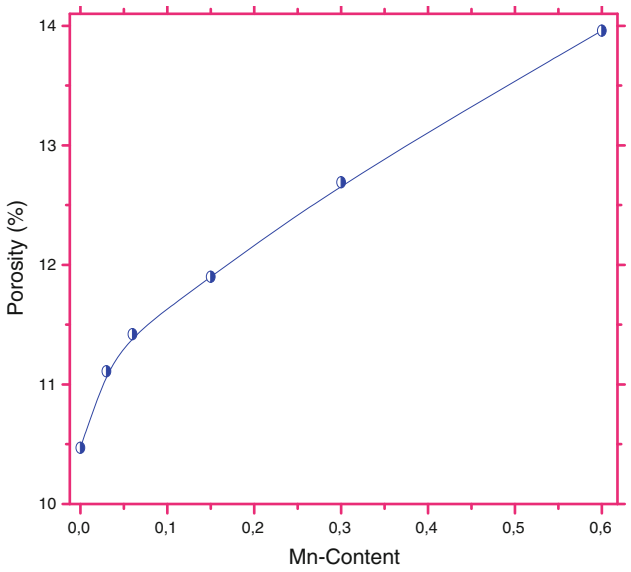

Fig. 8 Variation of porosity with Mn-content for Bi-2223 system

the ISE behavior for the pure sample. Conversely, the IIC model is obtained to be the best model to define the hardness values of the Mn doped Bi-2223 samples showing the RISE nature. It is related to the fact that the suitability of the IIC model to the samples examined may arise from two main reasons: the first one is that the specimen does not offer resistance or undergo elastic recovery as postulated in the HK approach, PSR and EPD models, nonetheless undergoes the relaxation involving a release of the indentation stress away from the indentation site. This may lead to a larger indentation size, and hence lower H_v at low loads [24]. In contrast, secondly, the RISE behavior causes to undergo the plastic deformation in the crystals, showing that these samples are perfectly brittle and this is even the case of the ceramic samples studied.

3.2 The porosity analyses

Transport properties of the grain boundaries in the $Bi_{1.8}Pb_{0.4}Sr_2Mn_xCa_{2.2}Cu_{3.0}O_y$ superconducting systems are characterized by use of the density measurements. The density of the pure BSCCO system is approximately taken to be 6.302 g/cm^3 in the theoretical density calculations [25]. With the aid of the density results obtained from [12], we can examine the porosities described as the degree of granularity to discuss the strength of connection between superconducting grains. In this work, the porosity values of the studied samples are calculated by means of the two methods defined in [26]. The porosity values of Mn0, Mn1, Mn2, Mn3, Mn4 and Mn5 samples are found to be about 10.47, 11.11, 11.42, 11.90, 12.69 and 13.96, respectively. The variation of the computed porosities as a function of the Bi-2223 ceramics is given in Fig. 8. As seen from the figure that the porosity values enhance with the increment of the Mn inclusions inserted in the Bi-2223 system and in fact the Mn5 sample has the largest pores along with the weakest connection between the superconducting grains, presenting that why the mechanical properties of the samples studied restrain with the content.

4 Conclusions

In this study, the influence of Mn additives on the mechanical properties of $Bi_{1.8}Pb_{0.4}Sr_2Mn_xCa_{2.2}Cu_{3.0}O_y$ superconductors elaborated by the conventional solid-state reaction with $x = 0$, 0.03, 0.06, 0.15, 0.3 and 0.6 is examined by way of H_v measurement. The H_v results allow us to derive the mechanical properties of the superconducting samples using the Meyer's law, PSR, EPD, HK approach and the IIC model. The results obtained indicate that the Mn doped Bi-2223 samples exhibit the RISE nature whereas the pure sample shows the ISE behavior. Moreover, the proportional specimen resistance model, EPD model and HK approach fail to explain the mechanical properties of the $Bi_{1.8}Pb_{0.4}Sr_2Mn_xCa_{2.2}Cu_{3.0}O_y$ samples exhibiting the RISE feature, but the IIC model is the best fitted as compared to the load dependence of microhardness values. On the other hand, the HK approach is successful for the pure sample obeying the ISE behavior. Further, the Young's modulus and yield strength values decrease (enhance) with the increment of the applied load for the pure (Mn doped) samples. The porosity values deduced from the bulk density values are also analyzed for

the grain connectivity in the systems. The relationship between the mechanical properties and grain connectivity depicts that the decrease in the mechanical properties with the enhancement of the Mn content in the system stems from the degradation of the connectivity between superconducting grains. In other words, the mechanical properties of the pure sample exhibiting the ISE behavior are superior to that of the others.

References

1. E. Martinez, J. Romera, A. Lousa, J. Esteve, Appl. Phys. A **77**, 419 (2003)
2. J. Sun, L.F. Francis, W.W. Gerberich, Polym. Eng. Sci. **45**, 207 (2005)
3. B. Kaur, M. Bhat, F. Licci, R. Kumar, P.N. Kotru, K.K. Bamzai, Nucl. Instrum. Methods Phys. Res. **222**, 175 (2004)
4. M. Dogruer, Y. Zalaoglu, G. Yildirim, A. Varilci, C. Terzioglu, J. Mater. Sci: Mater. Electron. (2012). doi:10.1007/s10854-012-1051-8
5. O. Uzun, U. Kolemen, S. Celebi, N. Guclu, J. Eur. Ceram. Soc. **25**, 969 (2005)
6. Y. Yoshino, A. Iwabuchi, R. Onodera, A. Chiba, K. Katagiri, T. Shimizu, Cryogenics **41**, 505 (2001)
7. C. Terzioglu, J. Alloys Compd. **509**, 87 (2011)
8. U. Kolemen, O. Uzun, M. Yilmazlar, N. Guclu, E. Yanmaz, J. Alloys Compd. **415**, 300 (2006)
9. S. Cavdar, E. Deniz, H. Koralay, O. Ozturk, M. Erdem, A. Gunen, J. Supercond. Nov. Magn. (2012). doi:10.1007/s10948-012-1629-7
10. R. Awad, A.I. Abou Aly, M. Kamal, M. Anas, J. Supercond. Nov. Magn. **24**, 1947 (2011)
11. M. Dogruer, G. Yildirim, O. Ozturk, A. Varilci, N. Soylu, O. Gorur, C. Terzioglu, J. Mater. Sci. Mater. Electron. (2012). doi: 10.1007/s10854-012-0917-0
12. G. Yildirim, S. Bal, E. Yucel, M. Dogruer, M. Akdogan, A. Varilci, C. Terzioglu, J. Supercond. Nov. Magn. **25**, 381 (2012)
13. M. Dogruer, Y. Zalaoglu, A. Varilci, C. Terzioglu, G. Yildirim, O. Ozturk, J. Supercond. Nov. Magn. **25**, 961 (2012)
14. A.A. Elmustafa, D.S. Stone, J. Mech. Phys. Solids **51**, 357 (2003)
15. S.M. Khalil, J. Phys. Chem. Solids **64**, 855 (2003)
16. H.C. Ling, M.F. Yan, J. Appl. Phys. **64**, 1307 (1988)
17. J.B. Quinn, G.D. Quinn, J. Mater. Sci. **32**, 4331 (1997)
18. F. Fröhlich, P. Grau, W. Grellmann, Phys. Stat. Sol. A **42**, 79 (1977)
19. B.D. Michels, G.H. Frischat, J. Mater. Sci. **17**, 329 (1982)
20. Q. Ma, D.R. Clarke, J. Mater. Res. **10**, 853 (1995)
21. G.P. Upit, S.A. Varchenya, Phys. Status Solidi A **17**, 831 (1966)
22. C. Hays, E.G. Kendall, Metallurgy **6**, 275 (1973)
23. H. Li, R.C. Bradt, J. Mater. Sci. **31**, 1065 (1996)
24. K. Sangwal, Mater. Chem. Phys. **63**, 145 (2000)
25. X. Yang, T.K. Chaki, Supercond. Sci. Technol. **6**, 343 (1993)
26. R.R. Reddy, M. Murakami, S. Tanaka, P.V. Reddy, Physica C **257**, 137 (1996)